arXiv:cond-mat/0306712v2 [cond-mat.supr-con] 16 Oct 2003

Theory of the quasiparticle interference patterns in the pseudogap phase of the cuprate superconductors

T. Pereg-Barnea and M. Franz
Department of Physics and Astronomy, University of British Columbia, Vancouver, BC, Canada V6T 1Z1
(Dated: February 2, 2008)

A method is proposed to test for the nature of the pseudogap phase in cuprates using the recently developed technique of Fourier transform scanning tunneling spectroscopy. We show that the observed quasiparticle interference patterns depend critically on the quasiparticle coherence factors, making it possible to distinguish between the pseudogap dominated by superconducting fluctuations and by various particle-hole condensates.

Existence of the pseudogap phase, a non-superconducting phase with suppressed single particle density of states (DOS) [1], represents perhaps the most dramatic departure of cuprates from the Landau Fermi liquid BCS-Eliashberg paradigm believed to describe conventional low-T_c superconductors. Theoretical approaches to the pseudogap phenomenon in cuprates fall broadly into two classes. One school of though attributes it to the incipient superconducting order whose amplitude forms at $T^* > T_c$ but remains phase incoherent down to T_c [2, 3, 4, 5, 6, 7, 8, 9]. The other school ascribes the pseudogap to the formation of some other (static or fluctuating) order, usually in the particle-hole (p-h) channel [10, 11, 12, 13]. Progress in understanding the physics of cuprates, and perhaps other strongly correlated superconductors, depends on the successful determination of the origin of the pseudogap phenomenon.

In this Communication we propose a test for the nature of the pseudogap phase based on the study of the quasiparticle interference patterns that can be observed by means of Fourier transform scanning tunneling spectroscopy (FT-STS) [14, 15, 16]. The existing data, taken deep in the superconducting phase of $Bi_2Sr_2CaCu_2O_{8+\delta}$ (Bi-2212), exhibit distinctive patterns of peaks in the reciprocal space. These peaks disperse through the Brillouin zone in a manner consistent with the band structure deduced from the angle resolved photoemission spectroscopy (ARPES). In what follows we demonstrate that, contrary to the existing consensus, the patterns observed in FT-STS depend in a crucial way on the quasiparticle *coherence factors*. We show that the appearance of peaks at the particular positions is unique to the superconducting order, and reflects the pairing (p-p) character of the coherence factors. By contrast the interference patterns in a state with p-h ordering will be qualitatively different in that peaks appear at different $\mathbf{k}$-vectors or not at all. Our proposal consists of extending the FT-STS measurements into the pseudogap phase above T_c. Observation of patterns similar to those seen well below T_c would then imply that pseudogap is predominantly of superconducting origin. Observation of qualitatively different patterns discussed below would imply order of another type. Preliminary data [17] appear to support the former scenario.

The existing FT-STS results [14, 15] have been interpreted via the 'octet model' [18], illustrated in Fig. 1. This model asserts that the interference patterns arise due to the elastic quasiparticle scattering from random disorder between the regions in the Brillouin zone with high DOS. In a d-wave superconductor (dSC) these are situated at the ends of the banana-shaped contours of constant energy and lead to seven characteristic vectors $\mathbf{q}_i$. This octet model works remarkably well in describing the data and furthermore agrees with detailed numerical studies of the interference patterns [18, 19, 20]. Our first step will therefore be to understand how the interference pattern is formed in the superconducting phase.

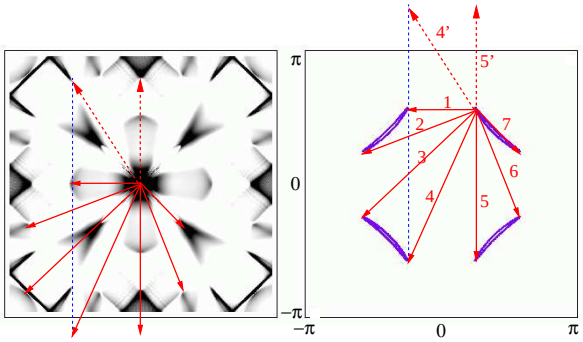

FIG. 1: Right: The banana shape contours of constant low energy around the nodes of the gap and seven vectors connecting their ends [14]. Left: Numerical evaluation of the Fourier transformed local density of states in Eq. (1) with $t' = 0.3t$, $\Delta_0 = 0.2t$, $\mu = -t$ and $\omega = 0.45\Delta_0$. In order to simulate the experimental resolution we filtered out the low-intensity background signal. The peaks disperse in a manner consistent with the octet model and the experimental data [14, 15].

The local density of states (LDOS) in a superconductor $n(\mathbf{r},\omega)$ is given by the particle-hole part of the Nambu Green's function. Within the usual $T-$matrix formulation [18, 19] the Fourier transformed LDOS modulation $\delta n(\mathbf{q},\omega)$ can be expressed as

$$\delta n = \mathrm{Im}\frac{1}{L^2}\sum_{\mathbf{k}}[G_0(\mathbf{k},\omega)\hat{T}(\mathbf{k},\mathbf{k}-\mathbf{q},\omega)G_0(\mathbf{k}-\mathbf{q},\omega)]_{11}, \tag{1}$$

where L is the linear size of the system and $G_0(\mathbf{k},i\omega) = [i\omega - \epsilon_{\mathbf{k}}\tau_3 - \Delta_{\mathbf{k}}\tau_1]^{-1}$ is the superconducting Green's function in the Nambu space. In what follows we consider

a model with dispersion $\epsilon_{\mathbf{k}} = -2t(\cos k_x + \cos k_y) - 4t' \cos k_x \cos k_y - \mu$ and a d-wave gap $\Delta_{\mathbf{k}} = \frac{\Delta_0}{2}(\cos k_x - \cos k_y)$. As shown by Capriotti *et al.* [20] the interference pattern measured in FT-STS for weak non-magnetic impurities is encoded in the quantity

$$\Lambda(\mathbf{q},\omega) = \frac{1}{L^2}\sum_{\mathbf{k}}[G_0(\mathbf{k},\omega)\tau_3 G_0(\mathbf{k}-\mathbf{q},\omega)]_{11}. \quad (2)$$

For simplicity we start by analyzing this case and we return to Eq. (1) with the full T-matrix shortly.

It is instructive to evaluate $\Lambda(\mathbf{q},\omega)$ in the low energy limit $\omega \ll \Delta_0$, where analytic results can be obtained. Inserting G_0 into Eq. (2) we find

$$\Lambda(\mathbf{q},i\omega) = \frac{1}{L^2}\sum_{\mathbf{k}} \frac{(i\omega+\epsilon_+)(i\omega+\epsilon_-) - \Delta_+\Delta_-}{(\omega^2+E_+^2)(\omega^2+E_-^2)}, \quad (3)$$

with $\epsilon_\pm = \epsilon_{\mathbf{k}\pm\mathbf{q}/2}$, $\Delta_\pm = \Delta_{\mathbf{k}\pm\mathbf{q}/2}$ and $E_\pm = \sqrt{\epsilon_\pm^2+\Delta_\pm^2}$. We now focus on the situation when both $\mathbf{k}\pm\frac{1}{2}\mathbf{q}$ are close to one nodal point; this should contribute to the peak in $\Lambda(\mathbf{q},\omega)$ at the vector labeled as $\mathbf{q}_7$ in the Fig. 1. Near this node we define a local coordinate system (k_1,k_2) and linearize the dispersion in the usual manner; $\epsilon_{\mathbf{k}} \to v_F k_1$ and $\Delta_{\mathbf{k}} \to v_\Delta k_2$, where v_F and v_Δ are quasiparticle velocities perpendicular and parallel to the Fermi surface, respectively. We find

$$\Lambda_{\rm lin} = \frac{1}{v_F v_\Delta}\int \frac{d^2k}{(2\pi)^2}\frac{-\omega^2+(k_1^2-k_2^2)-(\tilde{q}_1^2-\tilde{q}_2^2)}{[\omega^2+(\mathbf{k}-\tilde{\mathbf{q}})^2][\omega^2+(\mathbf{k}+\tilde{\mathbf{q}})^2]}, \quad (4)$$

where we have scaled the integration variables $k_1 \to k_1/v_F$, $k_2 \to k_2/v_\Delta$ and defined a new vector $\tilde{\mathbf{q}} = \frac{1}{2}(v_F q_1, v_\Delta q_2)$.

The above rescaling leads to our first useful insight: in the scaled frame of reference the contours of constant energy are concentric circles implying that vector $\mathbf{q}_7$ cannot have any special significance as far as the DOS is concerned. As we shall see below the peaks at $\pm\mathbf{q}_7$ arise solely due to the *coherence factors*, i.e. factors appearing in the numerator of Eqs. (3,4).

Integrals of the type appearing in Eq. (4) are familiar from the theory of massless relativistic Dirac fermions [21] and can be evaluated most conveniently by exploiting the Feynman parameterization [22]. The exact result is

$$\Lambda_{\rm lin}(\mathbf{q},\omega) = \frac{1}{2\pi v_F v_\Delta}\left[\left(\frac{\tilde{q}_2}{\tilde{q}}\right)^2 \mathcal{F}\left(\frac{\omega}{\tilde{q}}\right) - \frac{1}{2}\right],$$
$$\mathcal{F}(z) = 1 - \frac{z^2}{\sqrt{z^2-1}}\arctan\frac{1}{\sqrt{z^2-1}}. \quad (5)$$

For a given fixed energy ω function $\mathcal{F}(z)$ implies an inverse square root singularity in both the real and imaginary parts of $\Lambda_{\rm lin}(\mathbf{q},\omega)$ along an elliptic contour of constant energy given by $E_{\mathbf{q}} = 2\omega$ (here $E_{\mathbf{q}} = 2\tilde{q} \equiv \sqrt{v_F^2 q_1^2 + v_\Delta^2 q_2^2}$). More importantly this singularity is weighted by an angular factor $(\tilde{q}_2/\tilde{q})^2 = (v_\Delta q_2/E_{\mathbf{q}})^2$ producing the largest amplitude at the two ends of the ellipse, as illustrated in Fig. 2. These points of largest intensity coincide with $\pm\mathbf{q}_7$. We conclude that in this case the octet model works because of the *special BCS coherence factors* and not because of the DOS arguments. One can perform similar analyses for the internodal scattering and find a large response near some of the vectors $\mathbf{q}_i$ indicated in Fig. 1. Interestingly we find that the peak expected from the octet model near $\mathbf{q}_4$, which is absent in the experimental data [15], corresponds to an endpoint of a line of higher intensity.

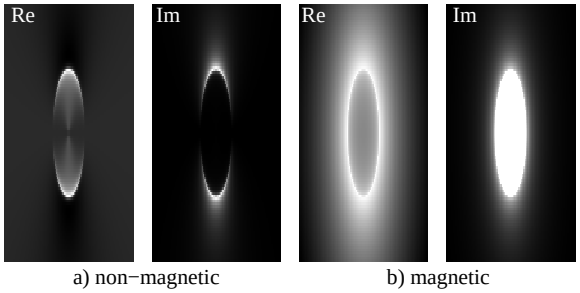

FIG. 2: Interference patterns in the single-node approximation. a) non-magnetic scattering Eq. (5), b) magnetic scattering Eq. (6). In both cases we use $v_F/v_\Delta = 4$. Note that the axes here represent the nodal coordinates q_1 (horizontal) and q_2 (vertical), rotated by 45° relative to Fig. 1.

One may now inquire what is the physics leading to the angular modulation of the singularity displayed in Eq. (5) and the consequent formation of the interference peaks in $\Lambda(\mathbf{q},\omega)$. A little thought reveals that the principal cause of this behavior is the particle-hole mixing. Charge is not a good quantum number in a superconductor; non-magnetic impurities couple to charge and this leads to strong angular modulation of the quasiparticle response as one travels along the contour of constant energy around the nodal point. To see this more clearly consider scattering by *magnetic* impurities. Magnetic impurities couple to quasiparticle *spin* and the latter remains a good quantum number in a superconductor. To describe this situation we replace τ_3 in Eq. (2) by $\tau_0 \equiv \mathbb{1}$. This reverses the sign in front of the $\Delta_+\Delta_-$ term in Eq. (3). Such a sign reversal has profound consequences for the response function $\Lambda(\mathbf{q},\omega)$ which can be again evaluated in the low energy limit near a single node. In this case the result is

$$\Lambda_{\rm lin}^{\rm mag}(\mathbf{q},\omega) = \frac{-1}{2\pi v_F v_\Delta}\left[i\pi + 2\mathcal{F}'\left(\frac{\omega}{\tilde{q}}\right) + \ln\left(\frac{\omega^2}{\lambda^2}\right)\right],$$
$$\mathcal{F}'(z) = \sqrt{z^2-1}\arctan\frac{1}{\sqrt{z^2-1}}, \quad (6)$$

with $\lambda \simeq \Delta_0$ a high energy cutoff. The inverse square root singularity of Eq. (5) is replaced by a cusp along $E_{\mathbf{q}} = 2\omega$ and, crucially, there is now no angular modulation. The interference patterns for magnetic disorder

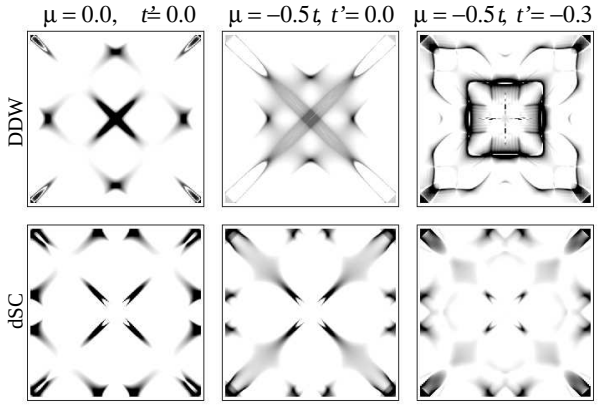

FIG. 3: Interference patterns in a DDW model of the pseudogap (top) compared with a dSC (bottom). In all figures $\omega = 0.3\Delta_0$ and $\Delta_0 = D_0 = 0.5t$.

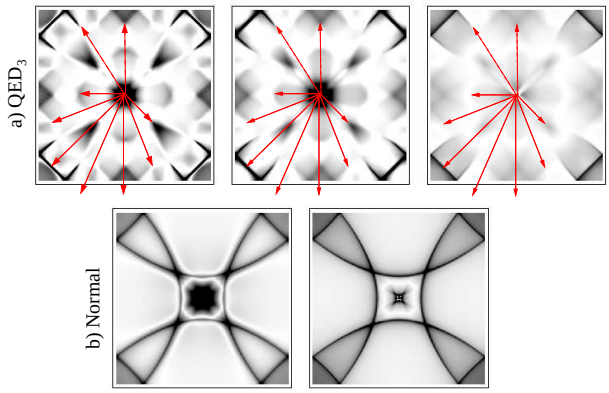

FIG. 4: a) Interference patterns within the QED$_3$ scenario with the anomalous dimension exponent $\eta = 0.0, 0.2, 0.4$ (left to right) and all other parameters as in Fig. 1. b) The FT-STS pattern calculated for a normal metal with the dispersion as in the dSC case and $\omega = 0.02t$ (left) and $\omega = 0.045t$ (right).

will exhibit *continuous lines* near the center of the BZ (Fig. 2b) and will be qualitatively different from those with scalar disorder, as already noted in Ref. [18].

The analysis of the low-energy limit of $\Lambda(\mathbf{q},\omega)$ thus shows that while the quasiparticle dispersion $E_{\mathbf{q}}$ determines the possible loci of strong interference, it is the coherence factors that determine the strength and select the actual location of the peaks on these loci.

To conclude our discussion of the superconducting state we evaluate $\delta n(\mathbf{q},\omega)$ given by Eq. (1) numerically with the full dispersion $\epsilon_{\mathbf{k}}$ and parameters relevant to Bi-2212. In Fig. 1 we use the full single-impurity, intermediate phase shift T-matrix, $\hat{T}(\omega) = T_0(\omega)\tau_0 + T_3(\omega)\tau_3$, as described in Ref. [23]. We find that experimental patterns are best reproduced by a particular value of the phase shift that yields $T_3(\omega) \approx -T_0(\omega)^*$. This choice effectively kills the analog of the $\Delta_+\Delta_-$ term in Eq. (3) and we are led to believe that in real systems this cancellation has a more fundamental cause, perhaps related to spatial fluctuations of the phase of Δ in a material with nanoscale electronic inhomogeneity [14, 15].

We now turn to the pseudogap state. If the pseudogap is due to an ordering in the p-h channel then the coherence factors will generally differ from those describing the superconductor. It is clear from the previous discussion that such coherence factors will produce qualitatively different interference patterns even if the DOS remains similar to that of a dSC. We now illustrate this general statement on the example of a d-density wave (DDW) state [12] that has been proposed to describe the pseudogap phase in cuprates. This is perhaps the most relevant example since for specially chosen parameters ($\mu = t' = 0$) the DOS in DDW state is *identical* to that in dSC. We show below that even in this case FT-STS patterns are qualitatively different.

Under the assumptions leading to Eq. (2) one can show that for DDW state the interference pattern is given by

$$\Lambda(\mathbf{q},\omega) = \frac{1}{L^2}{\sum_{\mathbf{k}}}' \mathrm{Tr}[G_0(\mathbf{k},\omega)(1+\tau_1)G_0(\mathbf{k}-\mathbf{q},\omega)], \quad (7)$$

where the prime denotes summation over the reduced Brillouin zone. The DDW propagator reads $G_0(\mathbf{k},i\omega) = [(i\omega - \epsilon'_{\mathbf{k}}) - \epsilon''_{\mathbf{k}}\tau_3 - D_{\mathbf{k}}\tau_2]^{-1}$, with $\epsilon'_{\mathbf{k}} = \frac{1}{2}(\epsilon_{\mathbf{k}} + \epsilon_{\mathbf{k}+\mathbf{Q}})$, $\epsilon''_{\mathbf{k}} = \frac{1}{2}(\epsilon_{\mathbf{k}} - \epsilon_{\mathbf{k}+\mathbf{Q}})$, $\mathbf{Q} = (\pi,\pi)$ and DDW gap $D_{\mathbf{k}} = \frac{D_0}{2}(\cos k_x - \cos k_y)$. One obtains

$$\Lambda(\mathbf{q},i\omega) = \frac{2}{L^2}{\sum_{\mathbf{k}}}' \frac{-\Omega_+\Omega_- + \epsilon''_+\epsilon''_- + D_+D_-}{(\Omega_+^2 + E_+^2)(\Omega_-^2 + E_-^2)}, \quad (8)$$

with $i\Omega_\pm = i\omega - \epsilon'_\pm$, $E_\pm = \sqrt{(\epsilon''_\pm)^2 + D_\pm^2}$ and '$\pm$' denoting $\mathbf{k} \pm \mathbf{q}/2$ as before. At low energies the spectrum of a DDW quasiparticle is Dirac-like with the node fixed at $(\pi/2, \pi/2)$. In this limit (8) can be again evaluated analytically by performing the nodal approximation. We find that the result is given by Eq. (6) with ω replaced by $\omega + \mu$ and v_Δ by v_D, the slope of the DDW gap. Thus, we find that at low energies DDW state will produce FT-STS patterns similar to those expected for dSC with *magnetic* scattering, characterized by continuous *lines* in the Brillouin zone as opposed to the sharp peaks. This is confirmed by a full numerical evaluation of Eq. (8) displayed in Fig. 3. The DDW patterns are markedly different from dSC even at half filling.

We now consider the class of theories which describe the pseudogap as an incipient superconducting gap. In these theories the long range superconducting order is destroyed above T_c but short range pairing correlations persist for $T_c < T < T^*$. Based on the above discussion we expect that such a pseudogap phase would inherit the FT-STS patterns characteristic of the superconducting phase since the coherence factors will locally retain their p-h character. As an example we consider the QED$_3$ theory of the pseudogap phase which has been proposed to describe a phase disordered dSC [7]. In this theory fluctuating phase of the SC order parameter produces an emergent massless U(1) gauge field which mediates long range interactions between the fermions. As a result the

fermion propagator becomes incoherent [8]:

$$G_0(\mathbf{k}, i\omega) = \frac{i\omega + \epsilon_{\mathbf{k}}\tau_3}{[\omega^2 + \epsilon_{\mathbf{k}}^2 + \Delta_{\mathbf{k}}^2]^{1-\eta/2}}, \qquad (9)$$

and exhibits a Luttinger liquid like dynamics at long distances with the sharp quasiparticle poles replaced by branch cut singularities characterized by the anomalous dimension exponent η. The latter is believed to be a small positive number but its exact value is a matter of debate [8]. Here we treat η as a parameter and show that the structure of FT-STS patterns is insensitive to its exact value. The QED_3 propagator lacks the off-diagonal part, reflecting the absence of true SC long range order.

One can again evaluate Eq. (2) with the QED_3 propagator (9) analytically within the single node approximation. For scalar disorder one finds a result similar to Eq. (5) with the square root singularity at $E_{\mathbf{q}} = 2\omega$ replaced by a weaker $1/(z^2-1)^{\frac{1}{2}-\eta}$ singularity. Thus, for $\eta < \frac{1}{2}$ we expect patterns similar to those in dSC. The numerical results, presented in Fig. 4, indeed show that the QED_3 interference patterns retain peaks at the same positions as in the SC phase but the peaks become smeared for larger η reflecting the incoherent nature of the fermionic excitations described by Eq. (9).

Finally, Fig. 4 displays the FT-STS patterns for the normal metallic state ($\Delta_0 = D_0 = 0$), which are expected to describe strongly overdoped cuprates.

In conclusion, we have shown here that the quasiparticle interference patterns seen in the FT-STS reveal the signatures of both the quasiparticle dispersion and, through their sensitivity to the quasiparticle coherence factors, the *nature of the underlying electronic order* present in the system. In particular, the latter determines the basic characteristic features of the interference patterns. We have demonstrated, by general arguments and detailed calculations within several relevant models, that the superconducting order is very special in that it alone produces patterns consistent with the experimental data. Based on this insight we have proposed a test for the nature of the pseudogap phase in cuprates using FT-STS. If the pseudogap is due to fluctuating SC order, then the FT-STS patterns above T_c should remain qualitatively the same as those below T_c. If, on the other hand, the pseudogap is due to static or fluctuating order in the p-h channel, such as SDW, CDW or DDW, the patterns above T_c should be *qualitatively different*, generally exhibiting continuous lines or peaks at different positions.

As mentioned above preliminary experimental data on Bi-2212 [17] show FT-STS patterns above T_c that are very similar to those found deep in the SC phase [14, 15, 16], suggesting that the pseudogap state is of predominantly superconducting origin. One may ask how robust is this identification of the pseudogap state, provided that the experimental data [17] can be reproduced. Our analysis indicates that the p-p nature of superconducting correlations plays critical role in formation of the patterns observed experimentally. Furthermore, despite significant effort, we were unable to construct a model with instability in p-h channel that would mimic these patterns. Therefore, we must conclude that data of Yazdani and co-workers [17], if correct, place very strong constraints on the nature of the pseudogap state in cuprates.

The authors are indebted to J.C. Davis, T. Davis, J. Hoffman, D.-H. Lee, S. Sachdev, D.E. Sheehy, O. Vafek, Z. Tešanović and A. Yazdani for discussions and correspondence. This work was supported by NSERC, CIAR and the A.P. Sloan Foundation.

[1] T. Timusk and B.W. Statt, Rep. Prog. Phys. **62**, 61 (1999).
[2] V.J. Emery and S.A. Kivelson, Nature **374**, 434 (1995).
[3] M. Randeria, *Varenna Lectures* (cond-mat/9710223).
[4] M. Franz and A.J. Millis, Phys. Rev. B **58**, 14572 (1998).
[5] L. Balents, M.P.A. Fisher and C. Nayak, Phys. Rev. B **60**, 1654 (1999).
[6] Q. Chen, K. Levin and I. Kosztin, Phys. Rev. B **63**, 184519 (2001).
[7] M. Franz and Z. Tešanović, Phys. Rev. Lett. **87**, 257003 (2001).
[8] M. Franz, Z. Tešanović and O. Vafek, Phys. Rev. B **66**, 054535 (2002).
[9] R. B. Laughlin, cond-mat/0209269.
[10] S.C. Zhang, Science **275**, 1089 (1997).
[11] C.M. Varma, Phys. Rev. Lett. **83**, 3538 (1999).
[12] S. Chakravarty, R.B. Laughlin, D.K. Morr, and C. Nayak Phys. Rev. B **63**, 094503 (2001)
[13] M. Vojta, Y. Zhang, and S. Sachdev, Phys. Rev. B **62**, 6721 (2000).
[14] J. Hoffman, K. McElroy, D.-H. Lee, K.M Lang, H. Eisaki, S. Uchida, J.C. Davis, Science **297** 1148(2002).
[15] K. McElroy, R. W. Simmonds, J.E. Hoffman, D.-H. Lee, J. Orenstein, H. Eisaki, S. Uchida & J.C. Davis, Nature **422** 592(2003).
[16] C. Howald, H. Eisaki, N. Kaneko, M. Greven, and A. Kapitulnik, Phys. Rev. B **67**, 014533 (2003).
[17] M. Vershinin, S. Misra, Y. Abe, Y. Ando and A. Yazdani Bull. Am. Phys. Soc. V48, Part 1, 372 (2003); A. Yazdani, private communication.
[18] Q.-H. Wang and D.-H. Lee, Phys. Rev. B **67**, 020511(2003).
[19] A. Polkovnikov, S. Sachdev and M. Vojta, cond-mat/0208334.
[20] L. Capriotti, D.J. Scalapino and R.D. Sedgewick, cond-mat/0302563.
[21] See e.g. M. E. Peskin and D. V. Schroeder, *An Introduction to Quantum Field Theory*, Addison-Wesley 1995.
[22] See e.g. Appendix B in Ref. [8].
[23] A.V. Balatsky, M.I. Salkola and A. Rosengren, Phys. Rev. B **51**, 15547 (1995).